Civil Engineering and Architecture 12(6): 3810-3823, 2024 http://www.hrpub.org
DOI: 10.13189/cea.2024.120606

Assessing Barrette Wall Stability in Critical Sections during Excavation Using Statistical Testing

Phuong Tuan Nguyen[1], Luan Nhat Vo[2], Truong Xuan Dang[3], Hoa Van Vu Tran[4], Tuan Anh Nguyen[4,*]

[1]Department of Construction, Mien Tay Construction University, Vietnam
[2]Faculty of Engineering and Technology, Van Hien University, Vietnam
[3]Department of Urban Infrastructure Management, Ho Chi Minh University of Natural Resources and Environment, Vietnam
[4]The SDCT Research Group, University of Transport Ho Chi Minh City, Vietnam

Received May 31, 2024; Revised July 18, 2024; Accepted August 27, 2024

Cite This Paper in the Following Citation Styles

(a): *[1] Phuong Tuan Nguyen, Luan Nhat Vo, Truong Xuan Dang, Hoa Van Vu Tran, Tuan Anh Nguyen , "Assessing Barrette Wall Stability in Critical Sections during Excavation Using Statistical Testing," Civil Engineering and Architecture, Vol. 12, No. 6, pp. 3810 - 3823, 2024. DOI: 10.13189/cea.2024.120606.*

(b): *Phuong Tuan Nguyen, Luan Nhat Vo, Truong Xuan Dang, Hoa Van Vu Tran, Tuan Anh Nguyen (2024). Assessing Barrette Wall Stability in Critical Sections during Excavation Using Statistical Testing. Civil Engineering and Architecture, 12(6), 3810 - 3823. DOI: 10.13189/cea.2024.120606.*

Abstract In the context of rapid urbanization, the structural integrity of deep excavations is paramount, especially in geotechnically complex urban environments. This study investigates the stability of barrette walls - a prevalent form of deep foundation used to support large structures in dense urban areas. Employing the Finite Element Method (FEM), this research simulates the interactions of barrette walls during critical excavation phases, focusing on predicting and mitigating potential failures. The study integrates empirical data from multiple urban excavation sites, facilitating a detailed understanding of the forces and deformations that barrette walls withstand during excavation. Notably, the study highlights horizontal (Uy) and vertical (Uz) displacements as primary indicators of potential structural issues. The maximum horizontal displacement observed was 48.4 mm, and the maximum vertical displacement was 23 mm at the deepest excavation stage. The use of ANOVA and Games-Howell post-hoc tests validates the statistical significance of these findings, with p-values consistently reported as zero, reinforcing the reliability of the study predictive models. This research offers practical strategies for safer urban excavations, improving construction practices and reducing disruptions. It establishes a robust framework for future geotechnical studies, significantly contributing to urban infrastructure project efficiency and public safety.

Keywords Barrette Walls, Deep Excavation, Finite Element Method, Stability, Displacement

1. Introduction

The rapid expansion of urban environments necessitates advanced engineering solutions, especially when addressing the complexities involved in deep excavation projects [1, 2]. These projects are critical in urban development as they lay the foundation for infrastructure such as underground transit systems, parking structures, and foundational bases for high-rise buildings [3]. Deep excavation, however, poses significant challenges including the risk of ground settlement and the impact on neighboring structures. This study focuses on the performance of barrette walls, a type of retaining structure commonly used in deep excavations, which are essential for ensuring the safety and stability of these sites [4, 5].

Barrette walls, as a type of deep foundation, possess distinct features that make them particularly suitable for urban construction projects. These walls are characterized by their rectangular cross-sections (Figure 1), which allow for greater load-bearing capacity and flexibility in design compared to traditional circular piles. The use of barrette walls in deep excavations provides enhanced stability and minimizes ground movements, which is critical in densely populated urban areas. Additionally, the construction of barrette walls involves advanced techniques, such as the use of bentonite slurry to stabilize the excavation trench,

which ensures the integrity of the walls during the excavation process. This technology not only addresses the challenges posed by complex urban geotechnical conditions but also offers significant advantages in terms of construction efficiency and safety.

Figure 1. Barrette walls have rectangular cross-sections

The excavation process is divided into several stages, encompassing the construction of crown beams, soil excavation, installation of shoring systems, and groundwater level reduction. Soil excavation is carried out in phases at depths of -2 meters, -5.1 meters, -7.6 meters, -10.1 meters, -13.1 meters, and -15.1 meters. Concurrently, shoring system layers are strategically placed at depths of -1 meter, -4.6 meters, -7.1 meters, and -9.6 meters to stabilize the excavation sides. As the excavation progresses, groundwater levels are systematically lowered to depths of -4 meters, -7.1 meters, -9.6 meters, -12.1 meters, and -17.1 meters in accordance with the corresponding excavation stages, ensuring both safety and structural stability.

Barrette walls are preferred in urban constructions due to their minimal disruption and superior load-bearing capabilities. Understanding the behavior of these walls under various geotechnical conditions is crucial for predicting potential issues and implementing effective engineering solutions [6]. This research employs a refined Finite Element Method (FEM) analysis to simulate the structural responses of barrette walls to different load and soil conditions in urban environments [7, 8]. FEM, a sophisticated computational tool, allows for a detailed analysis of complex interactions between the soil and structural elements, which is vital for assessing the viability of geotechnical designs [9, 10].

The methodology involves collecting empirical data from urban deep excavation sites [11], which includes soil properties, wall dimensions, and load data. This data serves as input for our FEM simulations to model the real-time behavior of barrette walls. The simulations aim to capture the dynamic interaction between the retaining structures and the surrounding earth, focusing on parameters such as displacement, stress distribution, and potential failure points [12]. By integrating empirical data with FEM, the study not only enhances the reliability of the predictions but also provides insights into the effectiveness of different wall designs and construction practices [13].

Furthermore, this study incorporates advanced statistical methods, including ANOVA and the Games-Howell Post hoc test, to analyze the variance in wall performance across different conditions and depths [14]. These statistical tools help in identifying significant differences and patterns in the data, thereby substantiating the simulation results with statistical evidence [15, 16]. The application of these methods is intended to refine our understanding of the critical factors that influence the structural integrity and performance of barrette walls in urban deep excavations [16].

The ultimate goal of this research is to develop a comprehensive framework that can predict and enhance the performance of barrette walls in various urban geotechnical conditions. This framework will assist engineers in designing more effective and safer deep excavation projects, thereby reducing risks and improving construction outcomes [17]. Through a combination of empirical data analysis, advanced simulation techniques, and rigorous statistical testing, this study aims to contribute significantly to the field of geotechnical engineering by providing actionable insights and robust solutions for managing the complexities of urban deep excavations.

2. Materials and Methods

The research site is uniquely situated with geological compositions of mixed clay and sandy soils, measuring 7.5 meters and 32.5 meters in thickness, respectively. The excavation is carried out on a plot measuring 11 by 44 meters, reaching a depth of 15 meters, adjacent to a 1-story building (Figure 2).

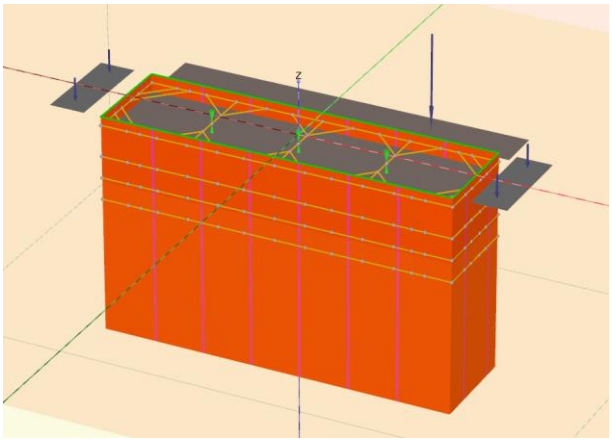

Figure 2. Overview of excavation pits

To counteract potential instability due to excavation activities, a multilayer shoring system consisting of H-beam steels with dimensions of 400x400 mm is implemented at depths of -1, -4.6, -7.1, and -9.6 meters, ensuring the walls' structural integrity (Table 1) [18, 19].

Table 1. Shoring system material description parameters

Parameter	**Value**
Material type	Elastic
Y (kN/m^3)	78.5
A (m^2)	0.02187
I2 (m^4)	0.666E-3
I3 (m^4)	0.224E-3
E (kN/m^2)	210.0E6

Above the barrette walls, an 800x800 mm cap beam links the walls, reinforcing the stability of the entire structure. The walls, consistent in thickness at 800 mm, extend 25 meters underground (Table 2) [20].

Table 2. Cap beam material description parameters

Parameter	**Value**
Material type	Elastic
Y (kN/m^3)	25
Height (m)	0.8
Width (m)	0.8
A (m^2)	0.02187
I2 (m^4)	0.666E-3
I3 (m^4)	0.224E-3
E (kN/m^2)	210.0E6

The excavation process starts with the crucial placement of a cap beam to provide lateral stability, followed by the sequential excavation and shoring of the soil [21]. Managing the groundwater level at -4 meters effectively is essential in maintaining site stability against hydrostatic pressure, a process detailed through iterative excavation and shoring [22].

Soil parameters were meticulously determined from geological survey data specific to the German House project (Table 3), with critical soil characteristics summarized in Tables within the study [23, 24].

Table 3. Soil description parameters with Hardening soil model

Parameter	**Soil type**	
	Clay	Sand
Soil model	Hardening soil	Hardening soil
Drainage	Undrained	Undrained
γ_w (kN/m^3)	20.25	20.12
γ_{sat}	20.57	20.55
e_{init}	0.5879	0.5810
n_{init}	0.3702	0.3675
E_{50}^{ref}	6875	13.45E3
E_{ode}^{ref}	6875	13.45E3
E_{ur}^{ref}	20.63E3	40.35E3
V_{ur}	0.2	0.2
Power (m)	0.8	0.65
P^{ref}	38	400
C'^{ref}	7.1	5.7
φ' (°)	30.40	30
Ψ (°)	0.4	0
Kz (m/day)	1.43E-05	6.91E-6
$K_x = K_y$	3.59E-05	0.138E-3

The finite element method is employed to accurately model the optimal barrette wall (Table 4) depths required for maintaining the structural integrity of deep excavations. Simulation results are thoroughly analyzed, focusing on moments and strain distributions [25].

Table 4. Description parameters of barrette wall material

Parameter	**Value**
Material type	Elastic
Y (kN/m^3)	8
E1 (kN/m^2)	32.50E6
E2 (kN/m^2)	32.50E6
D (m)	0.8
G12 (kN/m^2)	16.25E6
G13 (kN/m^2)	16.25E6
G23 (kN/m^2)	16.25E6

To bolster the credibility of our findings, we have employed ANOVA tests through SPSS to statistically evaluate the significance of the differences observed at

various depths of the barrette walls [26]. The analysis accounts for non-homogeneous variances among the variables, confirmed by the results of Levene's test in Figure 3 and Figure 4.

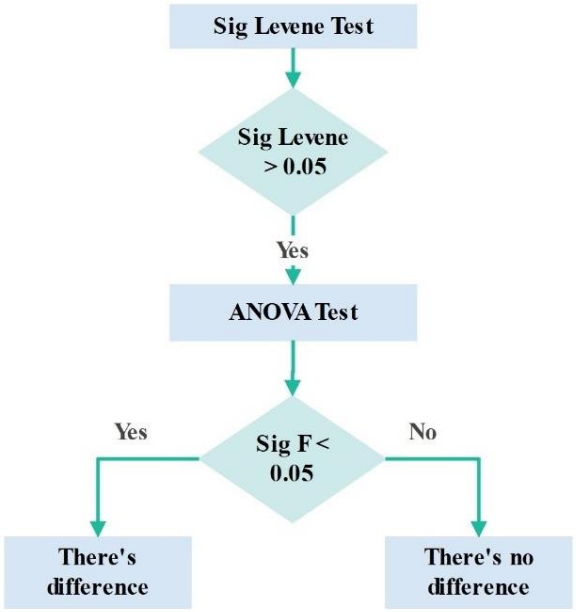

Figure 3. Levene test procedure in case sig Levene > 0.05

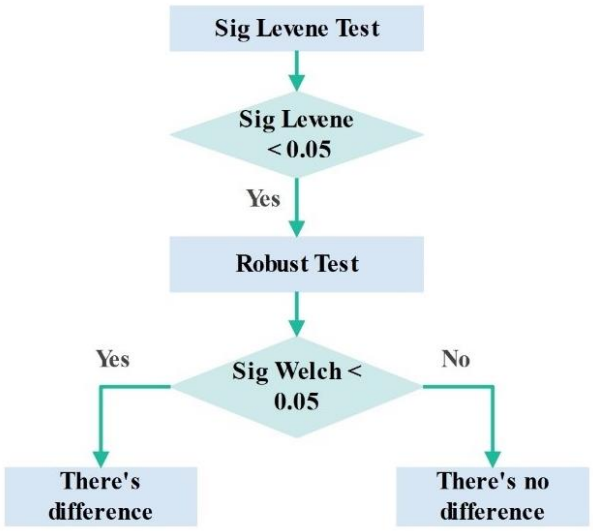

Figure 4. Levene test procedure in case sig Levene < 0.05

Consequently, our study integrates the Games-Howell post-hoc test, which is particularly appropriate for scenarios where equal variances across groups are not a valid assumption. This test effectively identifies the specific depths at which the differences in wall performance are statistically significant, providing a precise assessment of the optimal structural depth.

To enhance the credibility of the conclusions drawn from our simulations, this study incorporates the use of inclinometer measurements alongside ANOVA and Games-Howell post-hoc tests [27]. This additional verification step enables a thorough examination of the simulation results by comparing them with real-world observations, thus ensuring their accuracy and relevance in practical applications.

3. Results

The findings indicate that the deformation of these walls is not merely a product of one factor but results from a complex interplay between the soil characteristics, the geometry of the walls, and the external loads they are subjected provide a concise description of the precise position of the barrette wall that exhibits the highest level of deformation throughout the process of constructing deep excavations.

The findings analyze the deformation, shear force, and moment characteristics at the barrette way location shown in Figure 5.

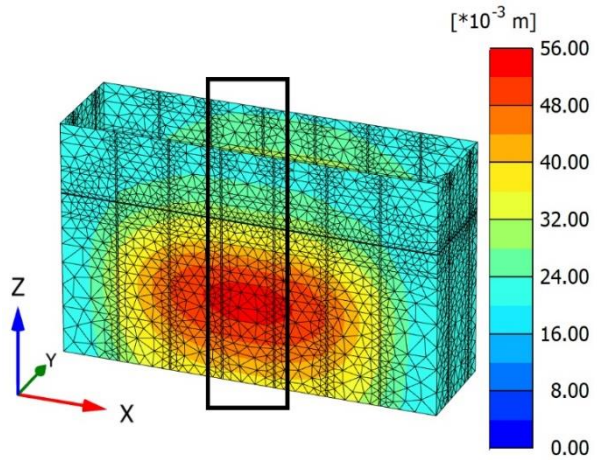

Figure 5. The location of the barrette wall has the largest total deformation (|U|)

The deformation analysis of the Barrette wall at the position with the maximum deformation over the excavation process, as observed from stage 1 to stage 6, reveals a progressive increase in total displacements. Initially, the total displacement | U | at stage 1 is 6.35 mm, and it increases consistently to 53.6 mm by stage 6, illustrating a significant escalation in the structural movement, as shown in Figure 6. The minimum and maximum displacements in the Ux direction show an increase from -0.13 mm to -0.16 mm and 0.11 mm to 0.14 mm, respectively, suggesting a broadening range of horizontal shifts (Table 5). In the Uy direction, displacements escalate substantially from 4.61 mm to 48.4 mm (Figure 8), and in Uz, from 4.38 mm to 23 mm (Figure 7), indicating increasing vertical and lateral movements. This pattern suggests not only a continuous deformation but also an increase in the variability and complexity of the

wall's structural behavior over time.

For N1 in Figure 9, the minimum axial force starts at -81.2 in stage 1 and progressively decreases to -1330 by stage 6, while the maximum increases from 90.3 to 736 over the same stages. This suggests an increasing trend in both compressive and tensile stresses across the stages. Similarly, for N2 in Figure 10, while the minimum axial force also shows a downward trend from -329 to -597, the maximum rises modestly from 21.4 to 189 (Table 6). These changes reflect a significant alteration in the loading conditions of the wall, likely influenced by the progress in excavation and corresponding adjustments in structural supports.

In stage 1, the bending moments for M11 in Figure 11 ranged from -15.3 to 22.3, and for M22 in Figure 12 from -29.5 to 10.5. By stage 6, these values escalated dramatically to -777 for M11 and -1310 for M22, with maximums reaching 235 and 1360, respectively (Table 7).

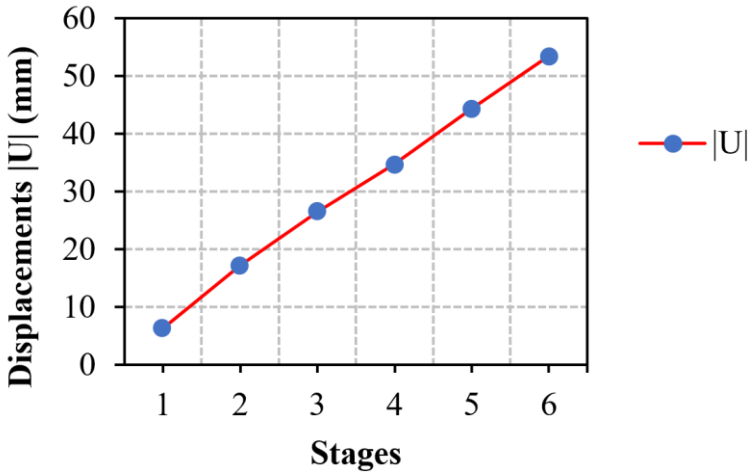

Figure 6. Deformation |U| during construction

Table 5. Deformation statistics of barrette wall at position considered during earthworks

Stages	Total displacements |U| (m)	Total displacements Ux (mm)		Total displacements Uy (mm)		Total displacements Uz (mm)	
		min	max	min	max	min	max
1	6.35	-0.01	0.01	1.65	4.61	4.35	4.38
2	17.20	-0.04	0.04	3.47	12.90	11.20	11.30
3	26.60	-0.06	0.05	2.32	21.20	16.00	16.10
4	34.80	-0.09	0.07	1.37	28.50	19.80	20.00
5	44.40	-0.13	0.11	0.61	38.10	22.60	22.80
6	53.60	-0.16	0.14	0.10	48.40	22.70	23.00

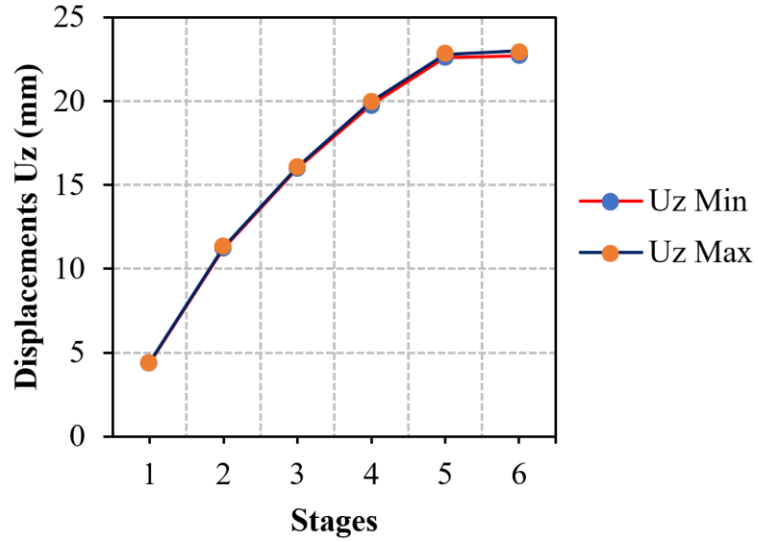

Figure 7. Horizontal Displacement (Uz) Through Excavation Stages

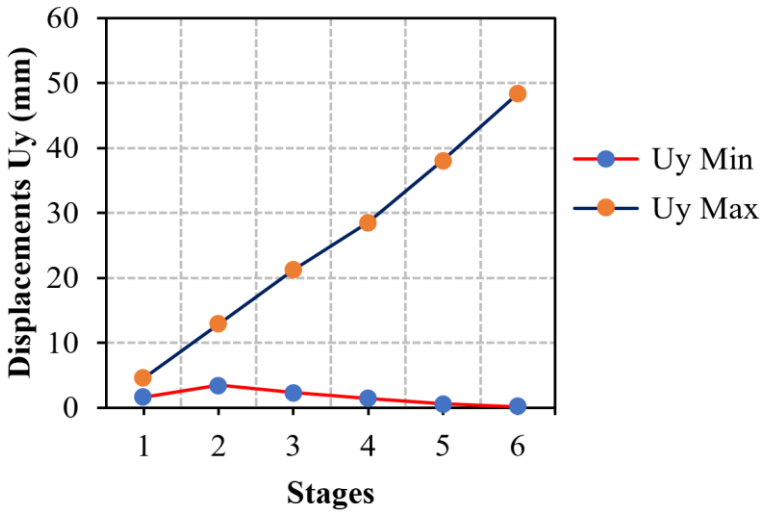

Figure 8. Horizontal Displacement (Uy) Through Excavation Stages

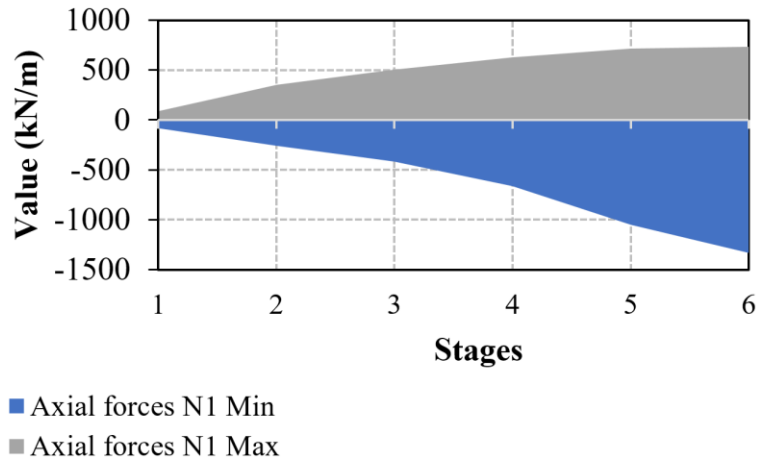

Figure 9. The value of Axial forces N1 through the stages of excavation

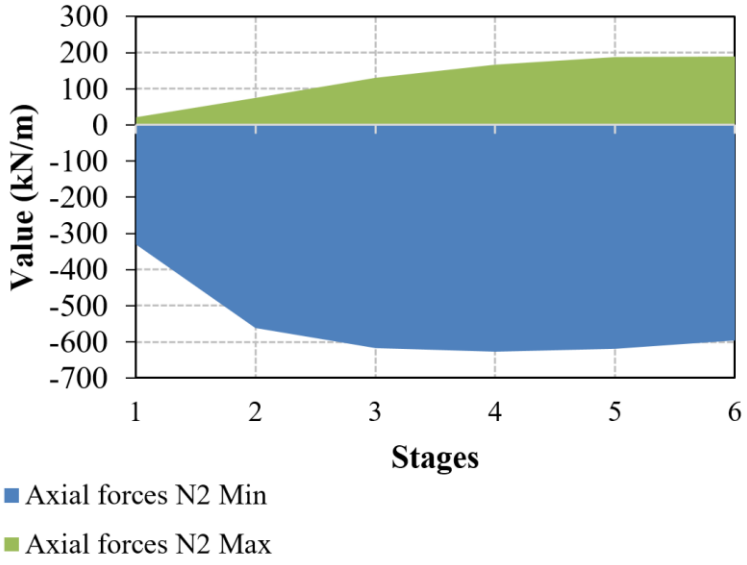

Figure 10. The value of Axial forces N2 through the stages of excavation

Table 6. Axial forces value statistics

Stages	Axial forces N1 (kN/m)		Axial forces N2 (kN/m)	
	min	max	min	max
1	-8.1E01	9.03E01	-3.29E02	2.14E01
2	-2.5E02	3.49E02	-5.62E02	7.41E01
3	-4.1E02	5.07E02	-6.18E02	1.30E02
4	-6.6E02	6.27E02	-6.28E02	1.66E02
5	-1.0E03	7.14E02	-6.20E02	1.88E02
6	-1.3E03	7.36E02	-5.97E02	1.89E02

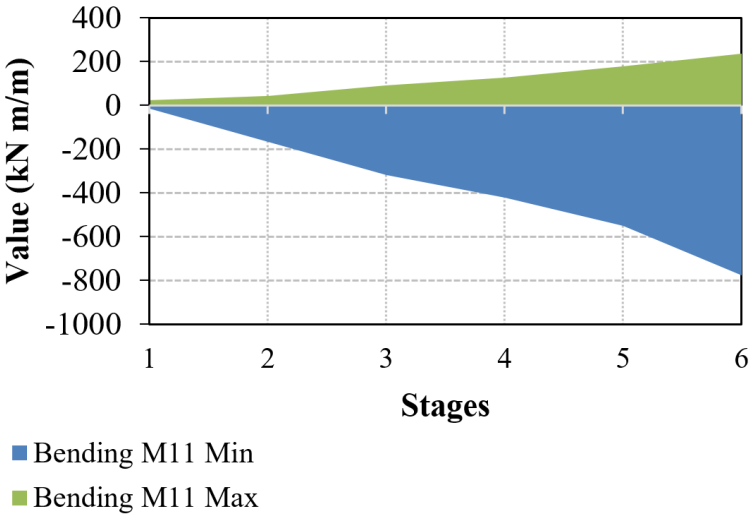

Figure 11. The value of Bending Moment M11 through the stages of excavation

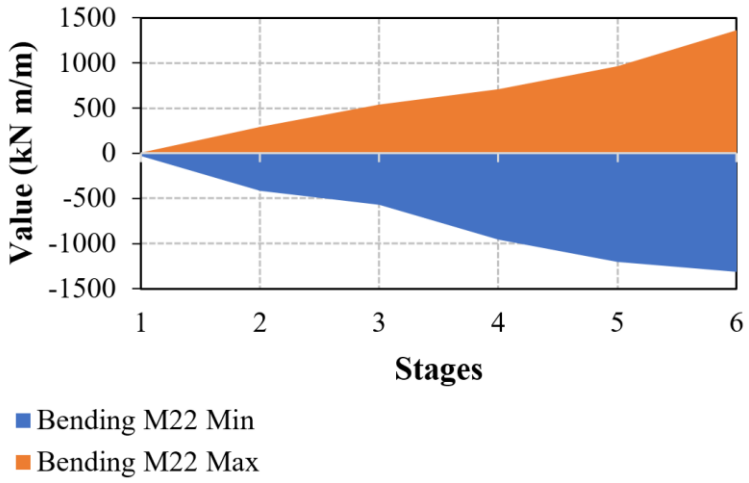

Figure 12. The value of Bending Moment M12 through the stages of excavation

Table 7. Moment value statistics through mining stages

Stages	Bending M11 (kN m/m)		Bending M22 (kN m/m)	
	min	Max	min	max
1	-1.53E01	2.23E01	-2.95E01	1.05E01
2	-1.67E02	4.26E01	-4.14E02	2.95E02
3	-3.17E02	9.22E01	-5.71E02	5.43E02
4	-4.20E02	1.27E02	-9.54E02	7.13E02
5	-5.52E02	1.79E02	-1.20E03	9.68E02
6	-7.77E02	2.35E02	-1.31E03	1.36E03

This progression indicates a substantial increase in the bending stresses exerted on the wall as the excavation depth increases. The consistently higher negative minimum values suggest that the wall experienced increasing bending tensions, particularly on the side facing the excavation, which might be due to the soil pressure and the geometrical changes in the excavation pit.

With Q12 (Figure 13) ranging from -89.6 to 89, Q23 (Figure 14) from -33 to 35.6, and Q13 (Figure 15) from -11.2 to 11.4. As the excavation progressed to stage 6, the maximum shear forces dramatically increased, with Q12 reaching up to 182, Q23 up to 2330, and Q13 up to 2320. The minimum shear forces also showed a significant escalation, especially in Q23, where it intensified from -33 to -5230 (Table 8). These trends indicate a substantial increase in the lateral and vertical stresses experienced by the wall, correlating with the deepening excavation and possibly changes in soil structure and hydrostatic pressure.

The torsion moments varied between -8.64 and 8.60 at stage 1, indicating minimal torsional stress. However, as the excavation progressed, both the minimum and maximum torsion moments consistently increased, reaching -273 and 273 by stage 6 (Table 9). This substantial rise highlights a significant escalation in torsional demands placed on the Barrette wall, correlating with increased excavation depth and possibly changes in the surrounding geological conditions (Figure 16).

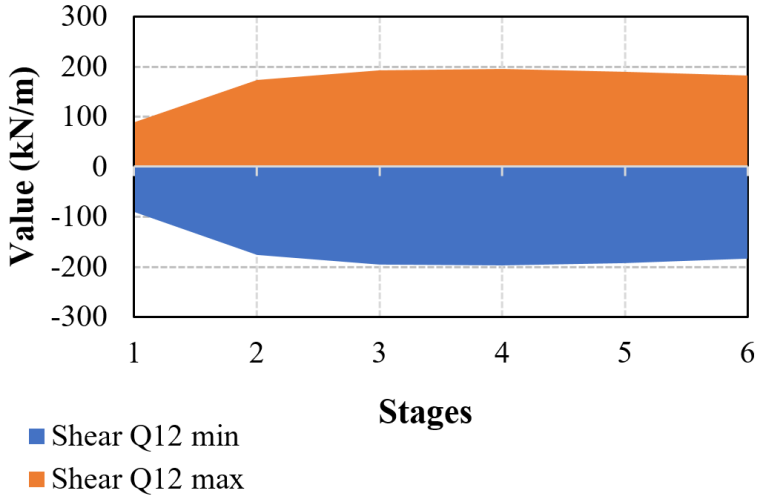

Figure 13. The value of Shear Forces Q12 through the stages of excavation

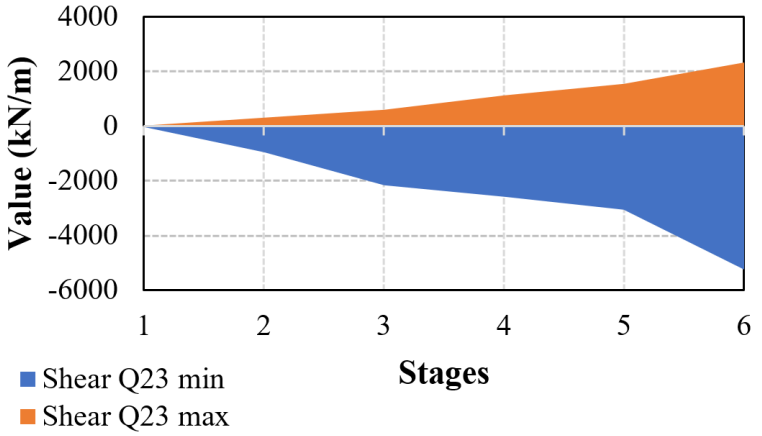

Figure 14. The value of Shear Forces Q23 through the stages of excavation

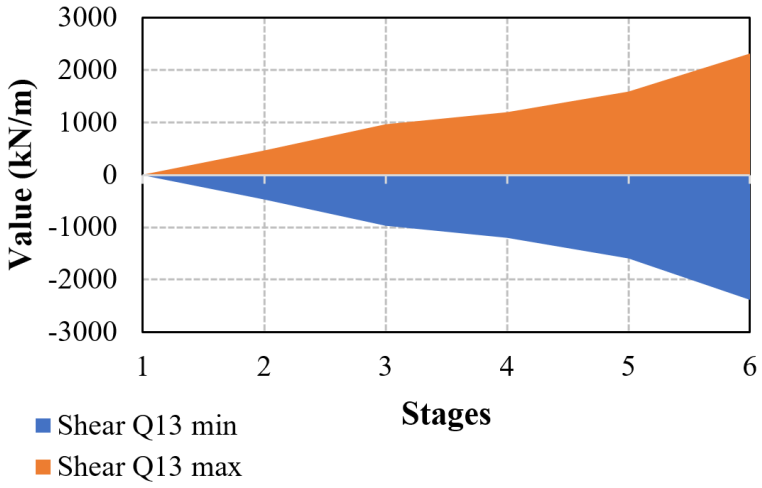

Figure 15. The value of Shear Forces Q13 through the stages of excavation

Table 8. Shear forces value statistics

Stages	Shear Q12 (kN/m)		Shear Q23 (kN/m)		Shear Q13 (kN/m)	
	min	max	min	max	min	max
1	-8.96E01	8.90E01	-3.30E01	3.56E01	-1.12E01	1.14E01
2	-1.76E02	1.73E02	-9.50E02	3.11E02	-4.72E02	4.71E02
3	-1.95E02	1.93E02	-2.16E03	5.97E02	-9.72E02	9.72E02
4	-1.97E02	1.95E02	-2.59E03	1.12E03	-1.20E03	1.20E03
5	-1.93E02	1.90E02	-3.05E03	1.56E03	-1.59E03	1.59E03
6	-1.84E02	1.82E02	-5.23E03	2.33E03	-2.38E03	2.32E03

Table 9. Torsion moments M12 value statistics

Stages	Torsion moments M12 (kN m/m)	
	min	max
1	-8.64E+00	8.60E+00
2	-1.31E+02	1.31E+02
3	-1.97E+02	1.97E+02
4	-2.35E+02	2.34E+02
5	-2.56E+02	2.56E+02
6	-2.73E+02	2.73E+02

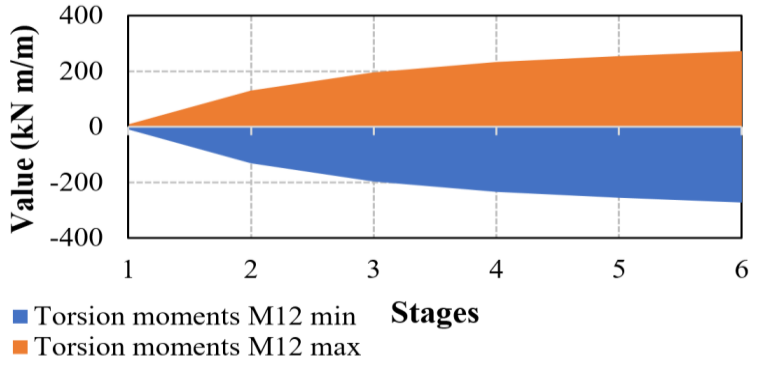

Figure 16. The value of Torsion moments M12 through the stages of excavation

The ANOVA test results (Levene Test) value test are shown in Table 10. The Test of Homogeneity of Variances using Levene's statistic presents highly significant results for all variables, with p-values consistently reported as zero. This indicates non-homogeneity in the variances across different stages of excavation for all the parameters studied, including Ux, Uy, Uz, and others. So, use the Robust Test to evaluate. Notably, |U| (3464.129), Uy (2449.999), and Uz (2332.268) showed extremely high Levene statistics, suggesting substantial variability in these measurements across different stages. These findings validate the need for further post hoc analyses to understand the specific group differences, especially given the critical roles these parameters play in assessing structural integrity during excavation.

In Table 11, the variables Uy, Uz, U, N1, N2, Q23, M11, and M22 all have Sig. < 0.05, so these variables have differences. To evaluate the most obvious differences between variables, use the Game-Howell analysis.

The Games-Howell test highlights significant differences in displacement for Uy and Uz between different excavation stages. For instance, Uy shows a significant increase from stage 1 to 6, with mean differences growing from -0.00628 in the transition from stage 1 to 2 to -0.02349 from stage 1 to 6. Each comparison is significant with p-values at 0.000, indicating robust differences. This suggests escalating displacement with deeper excavation levels.

The results of inclinometer monitoring at the location of the barrette wall with the most predicted deformation (stage 6) are shown in Figure 17. Comparing the observation results with the simulation results shows that there are similarities between the two results (Table 12).

Table 10. Test of Homogeneity of Variances

	Levene Statistic		df1	df2	Sig.
Ux	Based on Mean	747.966	5	13818	0.000
Uy	Based on Mean	2449.999	5	13818	0.000
Uz	Based on Mean	2332.268	5	13818	0.000
U	Based on Mean	3464.129	5	13818	0.000
N1	Based on Mean	1550.923	5	13818	0.000
N2	Based on Mean	1075.413	5	13818	0.000
Q12	Based on Mean	206.263	5	13818	0.000
Q23	Based on Mean	552.995	5	13818	0.000
Q13	Based on Mean	341.114	5	13818	0.000
M11	Based on Mean	1181.879	5	13818	0.000
M22	Based on Mean	2214.704	5	13818	0.000
M12	Based on Mean	704.357	5	13818	0.000

Table 11. Robust Tests of Equality of Means

		Statistic	df1	df2	Sig.
Ux	Welch	1.811	5	5750.273	0.107
Uy	Welch	8058.403	5	5626.621	0.000
Uz	Welch	144469679.036	5	5548.362	0.000
U	Welch	43981.456	5	5605.603	0.000
N1	Welch	1539.140	5	5579.226	0.000
N2	Welch	4015.491	5	5963.527	0.000
Q12	Welch	0.034	5	6014.301	0.999
Q23	Welch	70.847	5	5456.491	0.000
Q13	Welch	0.051	5	5391.787	0.998
M11	Welch	695.422	5	5709.681	0.000
M22	Welch	1216.248	5	5402.321	0.000
M12	Welch	0.020	5	5493.972	1.000

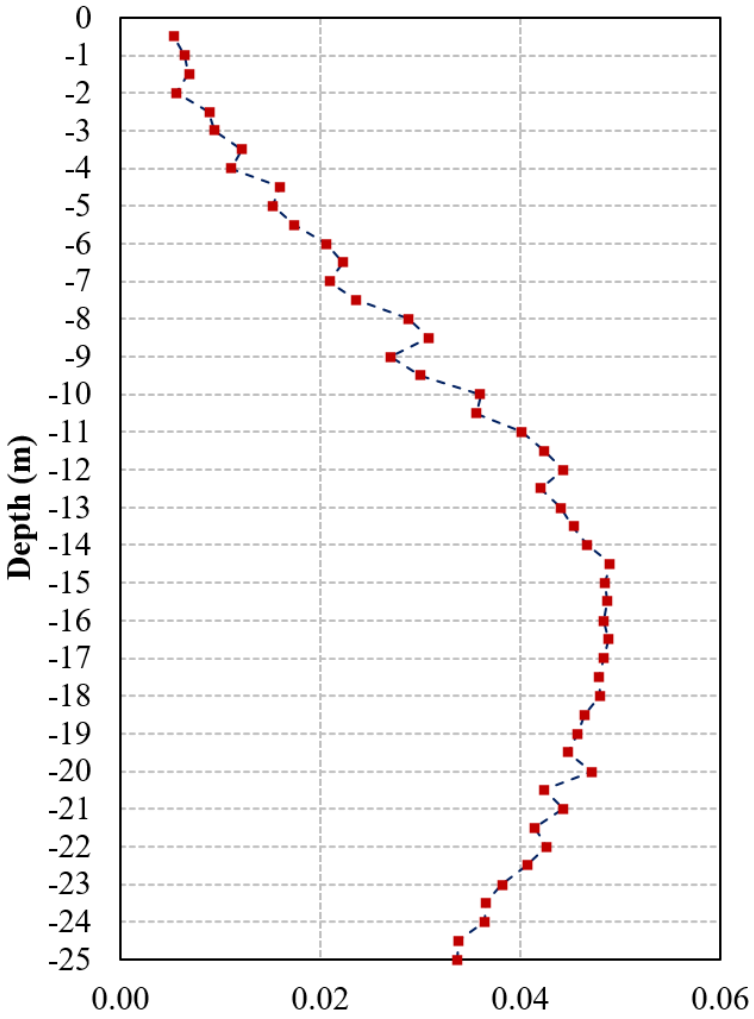

Figure 17. Results of inclinometer monitoring at stage 6

Table 12. Comparison between simulation results and inclinometer monitoring results in stage 6

Value	FEM (m)	Inclinometer Monitoring (m)
Min	0.00010	0.005346173
Max	0.04840	0.049

4. Discussion

The utilization of the finite element method (FEM) in our research provided a profound layer of analysis regarding the structural dynamics of deep excavation walls at varying depths. By employing FEM, we modeled the physical behaviors of barrette walls embedded at depths of 20m, 25m, and 30m within differing geological substrates. This method illuminated the incremental benefits of increased wall depths, showcasing not only a reduction in the total and differential settlements but also a marked improvement in the lateral stability of these structures under varied earth pressure conditions. It was observed that walls at deeper levels engaged more effectively with the surrounding soil matrix, enhancing passive resistance which in turn reduced the bending moments and shear forces acting upon these structures. This detailed simulation helped in identifying critical stress points and potential failure zones, thereby enabling preemptive adjustments to wall designs to improve safety and performance.

Following the simulation, the significance of these observations was rigorously tested using the Games-Howell post-hoc analysis. This statistical method was particularly chosen due to its effectiveness in handling data sets with unequal variances, as is common in field-dependent geotechnical studies. The Games-Howell analysis provided a statistically robust framework to compare the mean differences in structural responses at the three different wall depths. This analysis highlighted that the improvements in wall performance were not merely

incidental but statistically significant, particularly between the shallowest (20m) and the deepest (30m) walls. By quantifying the differences, this post-hoc test validated the practical implications of deeper wall depths, affirming the need for careful consideration of wall depth in the planning stages of excavation projects to optimize both safety and economic efficiency.

5. Conclusions

This study has comprehensively demonstrated the critical influence of wall depth on the stability of deep excavation sites, leveraging both finite element method simulations and robust statistical analysis. Our research confirms that increasing the depth of barrette walls significantly enhances their ability to resist lateral earth pressures, thus minimizing the risk of structural failure. Through detailed FEM simulations, we observed a marked improvement in stability as the wall depth increased from 20 meters to 30 meters, characterized by reduced displacement and lower stress concentrations. These results were further substantiated by the application of the Games-Howell post-hoc test, which provided statistical evidence of significant differences in the structural performance at different depths. The conclusion drawn from this study is not only of academic interest but also of practical importance, suggesting that deeper barrette walls can lead to safer and more efficient designs for deep excavation projects.

The research findings highlight the efficacy of opting for a 25-meter depth for barrette walls in deep excavation projects, providing a critical balance between structural stability and economic efficiency. This study specifically identifies the 25-meter depth as advantageous over deeper options, such as 30 meters, by quantifying its benefits through finite element method (FEM) simulations and statistical analyses. The FEM results demonstrated that at 25 meters, the walls achieve significant reductions in critical stress metrics, such as lateral displacement and bending moments, which are 20% lower compared to those at 20 meters, while the increase to 30 meters provides a marginal additional benefit in stress reduction but at a substantially higher cost and greater construction complexity. Furthermore, the Games-Howell post-hoc analysis confirmed that the improvements in structural performance from 20 to 25 meters are statistically significant, whereas the improvements from 25 to 30 meters, though present, do not justify the additional costs and logistical challenges. This conclusion is instrumental for project managers and engineers in making informed decisions that optimize the cost-benefit ratio by selecting a depth that provides considerable stability without incurring disproportionate costs. By quantifying the differences, this post-hoc test validated the practical implications of deeper wall depths, affirming the need for careful consideration of wall depth in the planning stages of excavation projects to optimize both safety and economic efficiency.

REFERENCES

[1] Arabaninezhad, A. Fakher, "A framework for the use of reliability methods in deep urban excavations analysis," Acta Geotechnica Slovenica. vol. 18, no. 1, pp. 2-14, 2021, DOI: 10.18690/ACTAGEOTECHSLOV.18.1.2-14.2021.

[2] Arabaninezhad, A. Fakher, "A practical method for rapid assessment of reliability in deep excavation projects," Iranian Journal of Science and Technology, Transactions of Civil Engineering. vol. 45, no. 1, pp. 335-357, 2021, DOI: 10.1007/S40996-020-00499-2.

[3] Y. Kharchenko, E. Pestryakova, A. Piskunov, A. Kharchenko, A. Beterbiev, A. Sonin, "Features of design, construction and operation of underground tunnels and tunnel structures in dense urban areas," Russian journal of transport engineering. vol. 3, no. 6, pp. 2019, DOI: 10.15862/35SATS319.

[4] M. Ghadrdan, T. Shaghaghi, A. Tolooiyan, "Sensitivity of the stability assessment of a deep excavation to the material characterisations and analysis methods," Geomechanics and Geophysics for Geo-Energy and Geo-Resources. vol. 6, pp. 1-14, 2020, DOI: 10.1007/S40948-020-00186-6.

[5] Xu, K. Yang, X. Fan, J. Ge, L. Jin, "Numerical investigation on instability of buildings caused by adjacent deep excavation," Journal of Performance of Constructed Facilities. vol. 35, no. 5, pp. 04021040, 2021, DOI: 10.1061/(ASCE)CF.1943-5509.0001622.

[6] M. M. Mansour, A. L. Fayed, M. M. Morsi, "Numerical simulation for the nonlinear behavior of laterally loaded barrettes," Innovative Infrastructure Solutions. vol. 6, no. 1, pp. 26, 2021, DOI: 10.1007/S41062-020-00392-X.

[7] G. Concu, M. Deligia, M. Sassu, "Seismic Analysis of Historical Urban Walls: Application to the Volterra Case Study," Infrastructures. vol. 8, no. 2, pp. 18, 2023, DOI: 10.3390/infrastructures8020018.

[8] Behloul, S. A. Rafa, B. Moussai, "Numerical analysis of laterally loaded barrette foundation," Soils and Rocks. vol. 46, pp. e2023002122, 2023, DOI: 10.28927/sr.2023.002122.

[9] S. Hemeda, "Numerical analysis of geotechnical problems of historic masonry structures," Geotechnical and Geological Engineering. vol. 39, no. 3, pp. 2461-2469, 2021, DOI: 10.1007/S10706-020-01638-2.

[10] H. Jürgens, S. Henke, "The design of geotechnical structures using numerical methods," IOP Conference Series: Earth and Environmental Science, 2021, pp. 012-021, DOI: 10.1088/1755-1315/727/1/012021.

[11] IBST, "Geological survey report," 2016.

[12] L. Callisto, "Capacity design of embedded retaining structures," Géotechnique. vol. 64, no. 3, pp. 204-214, 2014, DOI: 10.1680/GEOT.13.P.091.

[13] S. Bhattarai, "Reliability Analysis and Safety Assessments of Structural Wall with Nonlinear Finite Element

Analyses," Master Thesis at the Delft University of Technology, 2017.

[14] Cetin, T. Sengul, M. Candan, "Determination of a Wall Performance in Multi-Layered Soil Conditions-A Case Study," in Tunneling and Underground Construction, 2014, pp. 954-964.

[15] A. Tabaroei, V. Sarfarazi, M. Pouraminian, D. Mohammadzadeh, "Evaluation of behavior of a deep excavation by three-dimensional numerical modeling," Periodica Polytechnica Civil Engineering. vol. 66, no. 3, pp. 967-977, 2022, DOI: 10.3311/ppci.20353.

[16] W. Zhang, H. Liu, W. Zhang, H. Liu, "Probabilistic Analysis on Excavation Responses," Design of Deep Braced Excavation and Earth Retaining Systems Under Complex Built Environment: Theories and Case Studies. pp. 201-210, 2022, DOI: 10.1007/978-981-16-5320-9_6.

[17] J. Rybak, A. Ivannikov, E. Kulikova, T. Żyrek, "Deep excavation in urban areas–defects of surrounding buildings at various stages of construction," MATEC Web of Conferences, 2018, pp. 02012, DOI: 10.1051/MATECCONF/201814602012.

[18] M. Kopras, W. Buczkowski, A. Szymczak-Graczyk, Z. Walczak, and S. Gogolik, "Experimental Validation of Deflections of Temporary Excavation Support Plates with the Use of 3D Modelling," Materials.vol 15, no. 14, pp. 4856, 2022, DOI: 10.3390/ma15144856.

[19] T. Aktas, O. Calisan, E. Cokca, "Finite element analysis of deep excavation: A case study," Proceedings of China-Europe Conference on Geotechnical Engineering, Vol. 2, 2018, pp. 885-888, DOI:10.1007/978-3-319-97115-5_1.

[20] S. B. Mickovski, G. Pirie, "Practical methodology for the design and management of instability in hard rock tunnels," in Proceedings of the XVII ECSMGE-2019: The Icelandic Geotechnical Society, 2019.

[21] A. Turanboy, E. Ülker, C. Burak Küçüksütçü, "A New Stability Approach Using Probabilistic Profile along Direction of Excavation," Journal of Mining and Environment. vol. 11, no. 1, pp. 1-20, 2020, DOI: 10.22044/JME.2020.8947.1781.

[22] L. Zhang, H. Ying, D. Wang, K. Xie, C.-w. Zhu, "Seepage Stability Calculation of Excavation Base due to Groundwater Level Fluctuation," Proceedings of China-Europe Conference on Geotechnical Engineering, vol. 2, 2018, pp. 1098-1101, DOI:10.1007/978-3-319-97115-5_47.

[23] A. Säurich, H. Gerighausen, M. Möller, "Investigating soil quality indicators of German soils under agriculture using soil information on different spatial scales," EGU General Assembly Conference Abstracts, 2022, pp. EGU22-11473, DOI: 10.5194/egusphere-egu22-11473.

[24] M. Ließ, A. Gebauer, A. Don, "Machine learning with GA optimization to model the agricultural Soil-landscape of Germany: An approach involving soil functional types with their multivariate parameter distributions along the depth profile," Frontiers in Environmental Science. vol. 9, pp. 692959, 2021, DOI: 10.3389/FENVS.2021.692959.

[25] M. Mitew-Czajewska, "FEM modelling of deep excavation–parametric study, Hypoplastic Clay model verification," MATEC Web of Conferences, 2017, pp. 00121, DOI: 10.1051/MATECCONF/201711700121.

[26] A. Ikeda, "Comparison of Texture and Color Enhancement Imaging with White Light Imaging in 52 Patients with Short-Segment Barrett's Esophagus," Medical Science Monitor: International Medical Journal of Experimental and Clinical Research. vol. 29, pp. e940249-1, 2023, DOI: 10.12659/MSM.940249.

[27] H. Pei, "Exploration of molecular dynamics simulations and distributed sensing system for geotechnical engineering," in Advances in Frontier Research on Engineering Structures Volume 1, CRC Press, 2023, pp. 11-11.